

Thermo-optic properties of ceramic YAG at high temperatures

Hiroaki Furuse,^{1*} Ryo Yasuhara,² and Keiji Hiraga¹

¹Kitami Institute of Technology, 165 Koen-cho, Kitami, Hokkaido 090-8507, Japan

²National Institute for Fusion Science, 322-6 Oroshi-cho, Toki, Gifu 509-5292 Japan

*furuse@mail.kitami-it.ac.jp

Abstract: The thermo-optic coefficient dn/dT at 632.8 nm and thermal expansion coefficient α of transparent ceramic yttrium aluminum garnet (YAG) were measured between room temperature and 600 K. The data showed that dn/dT increases with temperature and α is in good agreement with that of single-crystal YAG. To the best of our knowledge, these are the first experimental data of the thermo-optic properties of highly transparent ceramic YAG above room temperature. We also present, using previously reported values measured below room temperature, fitting parameters for dn/dT that are valid over a wide temperature range (70–600 K) with an average error of 2.0%.

©2014 Optical Society of America

OCIS codes: (140.3380) Laser materials; (140.6810) Thermal effects; (160.4760) Optical properties.

References and links

1. A. Ikesue and Y. L. Aung, "Ceramic laser materials," *Nat. Photonics* **2**(12), 721–727 (2008).
2. T. Taira, "Re³⁺-ion doped YAG ceramic lasers," *IEEE J. Sel. Top. Quantum Electron.* **13**(3), 798–809 (2007).
3. M. Tsunekane and T. Taira, "High-power operation of diode edge-pumped, composite all-ceramic Yb:Y₃Al₅O₁₂ microchip laser," *Appl. Phys. Lett.* **90**(12), 121101 (2007).
4. R. M. Yamamoto, B. S. Bhachu, K. P. Cutter, S. N. Fochs, S. A. Lets, C. W. Parks, M. D. Rotter, and T. F. Soules, "The use of large transparent ceramics in a high powered, diode pumped solid-state laser," in *Conference on Advanced Solid-State Photonics (ASSP)*, Technical Digest (Optical Society of America, 2008), paper WC5.
5. H. Furuse, J. Kawanaka, N. Miyanaga, T. Saiki, K. Imasaki, M. Fujita, K. Takeshita, S. Ishii, and Y. Izawa, "Zig-zag active-mirror laser with cryogenic Yb³⁺:YAG/YAG composite ceramics," *Opt. Express* **19**(3), 2448–2455 (2011).
6. W. Koehnner, *Solid-State Laser Engineering* (Springer, 2006).
7. D. C. Brown, "Ultrahigh-average-power diode-pumped Nd:YAG and Yb:YAG lasers," *IEEE J. Quantum Electron.* **33**(5), 861–873 (1997).
8. R. L. Aggarwal, D. J. Ripin, J. R. Ochoa, and T. Y. Fan, "Measurement of thermo-optic properties of Y₃Al₅O₁₂, Lu₃Al₅O₁₂, YAlO₃, LiYF₄, LiLuF₄, BaY₂F₈, KGd(WO₄)₃, and KY(WO₄)₂ laser crystals in the 80–300 K temperature range," *J. Appl. Phys.* **98**(10), 103514 (2005).
9. D. C. Brown, "The promise of cryogenic solid-state lasers," *IEEE J. Sel. Top. Quantum Electron.* **11**(3), 587–599 (2005).
10. T. Y. Fan, D. J. Ripin, R. L. Aggarwal, J. R. Ochoa, B. Chann, M. Tilleman, and J. Spitzberg, "Cryogenic Yb³⁺-doped solid-state lasers," *IEEE J. Sel. Top. Quantum Electron.* **13**(3), 448–459 (2007).
11. Y. Sato and T. Taira, "The studies of thermal conductivity in GdVO₄, YVO₄, and Y₃Al₅O₁₂ measured by quasi-one-dimensional flash method," *Opt. Express* **14**(22), 10528–10536 (2006).
12. H. Yagi, T. Yanagitani, T. Numazawa, and K. Ueda, "The physical properties of transparent Y₃Al₅O₁₂: Elastic modulus at high temperature and thermal conductivity at low temperature," *Ceram. Int.* **33**(5), 711–714 (2007).
13. Y. Sato, J. Akiyama, and T. Taira, "Effects of rare-earth doping on thermal conductivity in Y₃Al₅O₁₂ crystals," *Opt. Mater.* **31**(5), 720–724 (2009).
14. Y. Sato and T. Taira, "Highly accurate interferometric evaluation of thermal expansion and dn/dT of optical materials," *Opt. Mater. Express* **4**(5), 876–888 (2014).
15. S. Geller, G. P. Espinosa, and P. B. Crandall, "Thermal expansion of yttrium and gadolinium iron, gallium and aluminum garnets," *J. Appl. Cryst.* **2**(2), 86–88 (1969).
16. K. L. Ovanesyan, A. G. Petrosyan, G. O. Shirinyan, and A. A. Avetisyan, "Optical dispersion and thermal expansion of garnets Lu₃Al₅O₁₂, Er₃Al₅O₁₂, and Y₃Al₅O₁₂," *Inorg. Mater.* **17**, 308–310 (1981).
17. T. K. Gupta and J. Valentich, "Thermal expansion of yttrium aluminum garnet," *J. Am. Ceram. Soc.* **54**(7), 355–356 (1971).

18. J. D. Foster and L. M. Osterink, "Index of refraction and expansion thermal coefficients of Nd:YAG," *Appl. Opt.* **7**(12), 2428–2429 (1968).
19. T. Y. Fan and J. L. Daneu, "Thermal coefficients of the optical path length and refractive index in YAG," *Appl. Opt.* **37**(9), 1635–1637 (1998).
20. R. Wynne, J. L. Daneu, and T. Y. Fan, "Thermal coefficients of the expansion and refractive index in YAG," *Appl. Opt.* **38**(15), 3282–3284 (1999).
21. R. Yasuhara, H. Furuse, A. Iwamoto, J. Kawanaka, and T. Yanagitani, "Evaluation of thermo-optic characteristics of cryogenically cooled Yb:YAG ceramics," *Opt. Express* **20**(28), 29531–29539 (2012).
22. V. Cardinali, E. Marmois, B. Le Garrec, and G. Bourdet, "Determination of the thermo-optic coefficient dn/dT of ytterbium doped ceramics (Sc_2O_3 , Y_2O_3 , Lu_2O_3 , YAG), crystals (YAG, CaF_2) and neodymium doped phosphate glass at cryogenic temperature," *Opt. Mater.* **34**(6), 990–994 (2012).
23. Yu. N. Barabanenkov, S. N. Ivanov, A. V. Taranov, E. N. Khazanov, H. Yagi, T. Yanagitani, K. Takaichi, J. Lu, J. F. Bisson, A. Shirakawa, K. Ueda, and A. A. Kaminskii, "Nonequilibrium acoustic phonons in $\text{Y}_3\text{Al}_5\text{O}_{12}$ -based nanocrystalline ceramics," *J. Exp. Theor. Phys. Lett.* **79**(7), 342–345 (2004).
24. G. Ghosh, *Handbook of Thermo-Optic Coefficients of Optical Materials with Application* (Academic Press, 1998).
25. L. G. DeShazer, S. C. Rand, and B. A. Wechsler, Laser crystals, in *Handbook of Laser Science and Technology, Vol. V: Optical Materials, Part 3*, M. J. Weber, ed. (CRC Press, 1987).
26. X. Xu, Z. Zhao, J. Xu, and P. Deng, "Thermal diffusivity, conductivity and expansion of $\text{Yb}_{3x}\text{Y}_{3(1-x)}\text{Al}_5\text{O}_{12}$ ($x=0.05, 0.1$ and 0.25) single crystals," *Solid State Commun.* **130**(8), 529–532 (2004).

1. Introduction

Rare-earth-doped yttrium aluminum garnet (YAG) is found in various optical devices including solid-state lasers and as a phosphor in solid-state lighting and scintillators owing to its excellent mechanical, thermal, and optical properties. In particular, Nd- and Yb-doped YAG are the most typical laser-active materials for high-average-power lasers and nonlinear optical devices. Currently, high-grade ceramic YAG of any size and dopant concentration can be commercially manufactured, and this is leading to rapid progress in solid-state laser materials science [1,2]. The advantages of heavy doping, large apertures, and composite structures have enabled many new ceramic-based laser concepts [3–5], and ceramic technology will be exploited in future developments of higher average-power lasers with higher pulse energies for next-generation laser material processing.

One of the primary obstacles in developing high-average-power laser systems is thermal problem that negatively affects the laser performance. The strong optical pumping process in a solid-state laser material associates with high heat generation, and consequently produces a significant temperature gradient in the material, which leads to thermal lensing, stress-induced birefringence, thermal aberrations, and eventually thermal stress fracture. Thus, the output power of solid-state lasers is mainly limited by thermal effects in the gain medium. To solve these problems and obtain output power required at a high performance, thermal analyses and well-designed laser systems are important.

The thermal conductivity K (W/mK), thermal expansion α (1/K), and thermo-optic coefficient dn/dT (1/K) are particularly relevant parameters for a thermal assessment of a laser medium. For example, the degree of thermal lensing, thermal-stress birefringence, and fracture limit can be evaluated using these parameters [6]. Accurate values are accordingly required for designing high-performance laser systems.

Previous studies on the thermal properties of YAG have considered various temperature ranges. The temperature dependence of K in single-crystal YAG at low temperatures (30–300 K) [7–10] and high temperatures (300–473 K) [11] has been reported. For ceramic YAG, Yagi *et al.* [12] measured K -value at 5–200 K and found that the values corresponded to those of single-crystal YAG between 150 K to room temperature. Sato *et al.* [13] reported the dependence of K on rare-earth Nd^{3+} and Yb^{3+} concentration for both single-crystal and ceramic YAG from room temperature to 473 K. Recently, they also measured α for single-crystal YAG from room temperature to 573 K using a high-resolution dilatometer [14]. Geller *et al.* [15] and Ovanesyan *et al.* [16] determined α values of single-crystal YAG using an X-ray diffraction method up to 1400 and 1273 K, respectively. Gupta and Valentich [17] studied α on both single-crystal and ceramic YAG for temperatures up to 1673 K, while Foster and

Osterink [18] simultaneously measured α and dn/dT of a Nd^{3+} :YAG single crystal using a Fizeau interferometer. The interferometry method has also been used to measure dn/dT of single-crystal [19,20] and ceramic [21,22] YAG at low temperature; dn/dT is evaluated from the fractional change in the interference fringe pattern in an optical path length. The majority of these studies at temperatures below room temperature were carried out for developing cryogenically cooled Yb^{3+} :YAG lasers, which have excellent spectroscopic and thermal properties [9,10]. There have been very few studies at high temperatures, especially on dn/dT , but the temperature dependence of these thermal parameters above room temperature is needed for designing high-power lasers operating above room temperature.

In this paper, we report α and dn/dT values of ceramic YAG at temperatures between 300 and 600 K, the range of which can be used for assessing the thermo-optic effects in ceramic YAG lasers operated above room temperature. To the best of our knowledge, this is the first study of the temperature dependence of dn/dT of ceramic YAG up to 600 K. The values obtained in this study are compared with published data, and we propose a fit for dn/dT that is valid over 73–600 K.

2. Experiment

Figures 1(a) and 1(b) show a photograph and the dimensions of the undoped ceramic YAG sample (Konoshima Chemical Co., Ltd.), respectively. YAG flats 10 mm in diameter were polished and diffusion bonded to each end of the 15.6-mm-long, 5-mm-diameter rod. We employed a Fizeau interferometer (Fig. 1(c)) to measure the temperature dependence of α and dn/dT ; details of the measurements can be found elsewhere [21]. The YAG sample was attached to a copper holder, set in a vacuum chamber, and heated at 10 K/min. The temperature of the copper holder was measured by a thermo-couple. A 632.8 nm He-Ne laser was used as the probe beam, and two Fizeau interferometers were formed with the reflected light: one with a vacuum path (signal A) and the other with the YAG path (signal B). To avoid interference at the outer surface of the ceramic YAG in the vacuum path, each surface was partially anti-reflection (AR) coated at the probe laser wavelength. The signals were separated by a half mirror, and the shift in the fringes due to a temperature variation was recorded with photodetectors. The values of α and dn/dT were evaluated as follows:

$$\alpha = \frac{1}{L_1} \frac{dL_1}{dT} \quad (1)$$

$$\frac{1}{nL_2} \frac{d(nL_2)}{dT} = \alpha + \frac{1}{n} \frac{dn}{dT} \quad (2)$$

where $L_1 = 15.6$ mm and $L_2 = 22.4$ mm are the vacuum and YAG path lengths, respectively, and $n = 1.829$ is the refractive index of YAG at 632.8 nm.

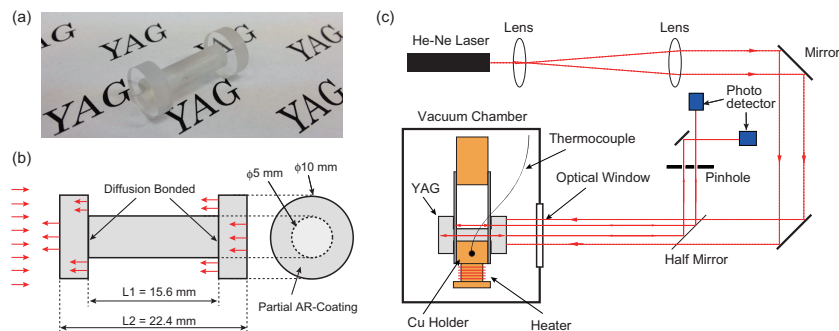


Fig. 1. (a) Photograph of the diffusion bonded ceramic YAG sample. (b) Sample configuration and optical path inside the sample. (c) Experimental setup of the interferometer.

Figure 2 shows an example of the measured photodiode intensity as a function of temperature around 435 K as well as sinusoidal fits. The phase shift in signals A and B over a 5-K temperature range (432.5–437.5 K) were evaluated to be $d(L_1) = 1.89\lambda$ and $d(nL_2) = 8.92\lambda$ ($\lambda = 632.8$ nm), respectively. These phase shift values were used to calculate α and dn/dT according to Eqs. (1) and (2). The same experiments were performed for temperatures of 300 to 600 K, and α and dn/dT were evaluated at 5-K intervals.

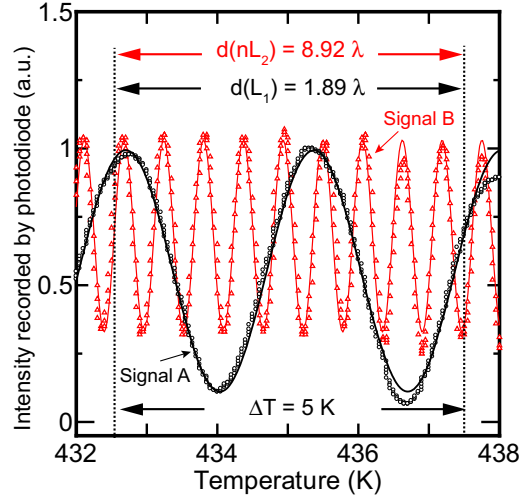


Fig. 2. Shift in the interference fringes in the vacuum path (signal A) and YAG path (signal B) over 432 to 438 K. Open symbols and solid lines represent the experimental values and sinusoidal fits, respectively.

3. Results and discussion

Figures 3(a) and 3(b) show the measured α and dn/dT values, respectively, of this work (black circles) and previous work (up to 300 K; red circles and blue squares) [21,22] along with single-crystal YAG values (green diamonds and triangles) [8,20], (up to 573 K; purple triangles) [14], and fits of α and dn/dT obtained from experimental data collected at low temperatures (dashed red lines) [21]. The measurements are repeated, and the measurement errors are evaluated to be $\pm 0.28 \times 10^{-6} \text{ K}^{-1}$ for α and $\pm 0.41 \times 10^{-6} \text{ K}^{-1}$ for dn/dT . The curve for α is by [21]

$$\alpha(T) = A \exp\left(-\frac{B}{T}\right) \quad (3)$$

where $A = 1.1434 \times 10^{-5} \text{ K}^{-1}$ and $B = 174.59 \text{ K}$. As can be seen in Fig. 3(a), the previously reported fitted curve shows concordance with our results; the average error between our experimental data and the fit is 1.7%. Thus, the fit can be applied to data for temperatures above room temperature. The dotted black and gray lines in Fig. 3(a) show the thermal expansion values of single-crystal YAG obtained from X-ray diffraction measurements [15,16]. Our experimental results are also in reasonable agreement with these values. The thermal expansion coefficients of ceramic YAG reported in [17] were smaller than those of single-crystal YAG because the ceramic YAG sample, sintered by hot pressing, had a low density (4.35 to 4.38 g/cm^3). Recent high-grade ceramic YAG has a higher density (4.55 g/cm^3) comparable to that of single-crystal YAG (4.56 g/cm^3) [23]. Therefore, we believe that the thermal expansion of ceramic YAG can be considered as equal to the value of single-crystal YAG. On the other hand, the thermal expansion of single-crystal [111]-cut YAG measured by a dilatometer has smaller values [14]. To discuss the expansion data between

single-crystal and ceramic YAG, we will conduct similar experiments for single-crystal YAG in the future.

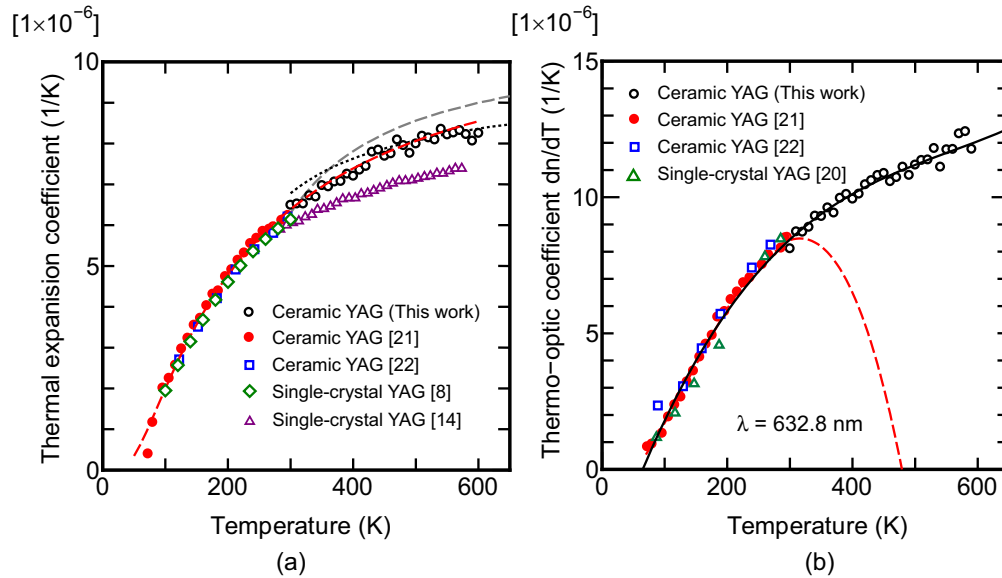


Fig. 3. Temperature dependence of the (a) thermal expansion coefficient α and (b) thermo-optic coefficient dn/dT of undoped YAG. Data is shown for our work on ceramic YAG (black circles), that reported elsewhere for ceramic YAG (red circles and blue squares) [21,22], and that reported for single-crystal YAG (green diamonds and triangles) [8,20] (up to 573 K; purple triangles) [14]. The dashed red lines are fits obtained from low-temperature data [21], the dotted black and dashed gray lines show single-crystal YAG data obtained from X-ray diffraction measurements [15,16], and the solid black line is the fit proposed in this work (Eq. (4)). All the dn/dT data shown were obtained using a 632.8 nm He-Ne laser.

Figure 3(b) shows that our experimental data for dn/dT at room temperature is in agreement with the polynomial fit reported in [21]. However, the fit is not valid for temperatures above room temperature. Here, we propose a new fit applicable to a temperature range of 70–600 K using experimental values at 632.8 nm below room temperature reported in [21]. This fit, like that in [21], is also based on a third-order polynomial:

$$\frac{dn}{dT}(T) = M_0 + M_1T + M_2T^2 + M_3T^3 \quad (4)$$

We obtained parameters of $M_0 = -3.96 \times 10^{-6}$, $M_1 = 6.75 \times 10^{-8}$, $M_2 = -1.06 \times 10^{-10}$, and $M_3 = 6.39 \times 10^{-14}$ by fitting this curve to the data. The average error between the experimental data and the fit is 2.0%, which indicates that Eq. (4) would be efficient and useful for designing laser systems that operate between 70 and 600 K. Note that this dn/dT fit is based on measurements performed with 632.8 nm probe wavelength. As the refractive index depends on wavelength, dn/dT values also change with wavelength. The dn/dT values of single-crystal YAG at various wavelengths (457.9–1064.2 nm) are given in [24,25] and decrease with increasing wavelength because of the wavelength-dependent refractive index dispersion.

For reference, the fitted values of α and dn/dT are listed in Table 1 along with the fractional change in the optical path length. In comparison to the value at room temperature, the fractional change in the optical path length increased by 17%, 29%, and 37% at 400, 500, and 600 K, respectively. Thus, the wave-front distortion including thermal lensing will be significantly larger for higher temperatures. In addition, the thermal conductivity of YAG is

predicted to be lower at temperatures above 300 K [7], and this should be addressed in developing high-power laser systems.

The doping and temperature dependences of the thermal expansion for single-crystal Yb^{3+} :YAG have been reported, and the thermal expansion increases with increasing temperature and Yb^{3+} doping concentration [13,26]. The thermo-optic coefficient will also change with the dopant and dopant concentration. Thus, for designing high-power laser systems, the doping concentration dependence of α and dn/dT for both Yb- and Nd-doped ceramic YAG will be measured.

Table 1. Fitted values of α and dn/dT for undoped ceramic YAG. The fractional change in the optical path length is also listed.

Temperature (K)	$\alpha (\times 10^{-6} \text{ K}^{-1})$	$dn/dT (\times 10^{-6} \text{ K}^{-1})$	$\alpha + \frac{1}{n} \frac{dn}{dT} (\times 10^{-6} \text{ K}^{-1})$
300	6.4	8.4	11.0
350	6.9	9.4	12.1
400	7.4	10.1	12.9
450	7.8	10.7	13.6
500	8.1	11.2	14.2
550	8.3	11.6	14.7
600	8.5	12.1	15.1

4. Conclusions

We have measured, for the first time, the values of α and dn/dT of ceramic YAG over a temperature range of 300–600 K. The thermal expansion coefficient was found to be in reasonable agreement with the experimental data of single-crystal YAG, and the thermo-optic coefficient at 300 K was consistent with a previously reported value. We demonstrated that the previously reported fit for ceramic YAG obtained from α data below room temperature can be used for temperatures up to 600 K. We have also presented for the first time fitting parameters for dn/dT that are valid over a wide temperature range (70–600 K) and have an average error of 2.0%. The fractional change in the optical path length increased by 17% at 400 K, as shown by a comparison with the value at 300 K. Therefore, the temperature dependence of α and dn/dT should be addressed especially in high-power lasers operating above room temperature, which have a large temperature distribution in the medium. We believe that the fits for α and dn/dT described by Eqs. (3) and (4) can be applied to analyze thermal effects in ceramic YAG and will be useful for designing high-average-power lasers operating under both cryogenic and high-temperature conditions.

In future work, we intend to measure the K , α , and dn/dT values of Yb^{3+} :YAG and Nd^{3+} :YAG at high temperatures and investigate the doping and temperature dependences. In addition, we will prepare a probe laser with a 1- μm wavelength for measuring dn/dT .

Acknowledgment

This work was performed with the support and under the auspices of the NIFS Collaboration Research Program (NIFS13KBAH006).